CRITICAL HEAT FLUX WITH SUBCOOLED FLOWING WATER IN TUBES FOR PRESSURES FROM ATMOSPHERE TO NEAR-CRITICAL POINT

Y. Chen, K. Bi, M. Zhao, C. Yang, K. Du
China Institute of Atomic Energy
P.O.Box 275(59) 102413 China
chenyz@ciae.ac.cn

ABSTRACT

In the previous investigation the critical heat flux experiment was performed in an Inconel tube of D_i = 7.98 mm to cover the pressures of 2.0 – 20.4 MPa. It was also performed in the tubes of D_i = 5.16, 8.05, 10.0 and 16.0 mm with pressures of 0.13 – 1.92 MPa. These data were calculated by the empiric correlations and a physical model. In the present study the experiment was extended to the Inconel tubes of D_i = 4.62 and 10.89 mm to cover the pressure of 1.7 – 20.6 MPa, mass flux of 454 – 4055 kg/m^{2}s and inlet water temperature of 110 – 354 K. In addition, the experiment of a tube of D_i = 2.32 mm was included, along with the data of D_i = 5.16 – 16.0 mm, to cover the pressure of 0.1 – 1.92 MPa, velocity of 1.47 – 23.3 m/s and local subcooling of 3.7 - 100.9 K. All these data were calculated by the modified empiric correlations and the physical model.

Keywords: Critical heat flux, near-critical pressure, subcooled

1. INTRODUCTION

Critical heat flux (CHF) is a major limit for the safety of nuclear reactors because the occurrence of CHF could lead to a failure of fuel element. During past six decades the CHF has been investigated extensively over the world, and a variety of prediction methods have been proposed, including the empiric correlations, the physical models and the look-up tables [1]. Because of the extreme complexity of the phenomena and the lack of adequate knowledge of the mechanisms, all these predictive methods are heavily relied on the experimental data. For the CHF of near-critical pressures, which is interest for the supercritical water-cooled reactors (SCWR), only a limited experimental data have been published in literature [2 – 5].

In China Institute of Atomic Energy (CIAE), a great number of CHF experimental data of subcooled flow water were obtained at lower pressure to support the designs of research reactors, including the CHF in the rod bundle and the annulus with heated from one side or both sides at steady-state or transient conditions [6]. They were the Heavy Water Research Reactor (HWRR), the High Flux Reactor (HFR) and the China Advance Research Reactor (CARR), and were first put into operation in 1957, 1980 and 2011, respectively. During this period, the CHF experiments were also performed in tubes of inner diameter of D_i = 5.16 – 16 mm at pressure of P < 2 MPa [7 - 8]. In recent years the research was extended to the near-critical pressure for the supercritical water-cooled reactors (SCWR). In the previous experiment some results of subcooled boiling CHF were obtained in an Inconel-625 tube of 7.98 mm in diameter with pressure of up to 20.0 MPa, and along with the data of D_i = 5.16 – 16 mm, the empiric correlations and a physical model were proposed [9 - 11]. In the present investigation the experiments were extended to the

Inconel-625 tubes of 4.62 and 10.89 mm in diameter to study further the CHF characteristics and the parametric trends. In addition, the experimental results of D_i = 2.32 mm was included, along with the data of D_i = 5.16 – 16 mm, to cover the ranges of P = 0.1 – 1.92 MPa and velocity of 1.47 – 23.3 m/s. All these data were formulated by the empiric correlations. The previous physical model with small modifications was verified for the pressure from atmosphere to the near-critical point and wide range of mass flux.

2. EXPERIMENTAL FACILITY AND PROCEDURE

For higher pressure, three Inconel-625 tubes were used: i) D_i = 4.62 mm, D_o = 6.5 mm and L_h = 0.5 m, ii) D_i = 10.89 mm, D_o = 12.7 mm and L_h = 1.1 m, and iii) D_i = 7.98 mm, D_o = 9.6 mm and L_h = 0.8 m (in the previous experiment). The water flowed upward through the inside of tube. This experiment was performed in a loop with the maximum pressure of beyond critical point. The test sections were heated by a DC supply with capacity of 7,000 A×65 V, and the preheater was heated by an AC supply.

For lower pressure, five stainless-steel tubes were used, including one with D_i = 2.32 mm and L_h = 0.09 m in the present experiment and four with D_i = 5.16, 8.05, 10.0 and 16.0 mm and different heated lengths in the previous experiment. This experiment was performed in an another test loop with maximum pressure of 2.0 MPa. The test sections were heated by a DC supply with capacity of 15000A×75V.

Major measurements of the parameters included: the outlet pressure, the flow rate, the inlet and outlet water temperatures of the test section, and the voltage and current across the heated tube. During experiment the deionized water was used. The pressure, the flow rate and the inlet water temperature were kept at constant, while the power to test section was increased with small step by step to approach the CHF. The onset of CHF was detected by photocells. Because the test section was heated uniformly, the CHF was always detected to occur near the end of heated length. The details of the experimental facilities and the procedures were described in references [9 - 11] for higher pressure and in references [6 - 8] for lower pressure.

3. EFFECTS OF MAJOR PARAMETERS ON THE CHF

3.1 Higher Pressure

The present experimental conditions are incorporated with the previous one, as listed in Table 1.

Table 1 The experimental conditions for higher pressure

D_i/L_h (mm/m)	P (MPa)	G (kg/m^2s)	$DT_{s,i}$ (K)	$DT_{s,o}$ (K)	q_{CHF} (MW/m^2)	Number of data
4.62/0.5	1.8 – 20.6	556- 4055	110 - 354	1 - 169	0.77 – 9.3	118
7.98/0.8	2.0 – 20.4	476- 1653	53 - 361	3 - 158	0.26– 4.95	193
10.89/1.1	1.7 – 20.0	454- 1144	169 - 345	4 - 141	0.92 – 3.3	56

Figure1 exemplifies the variations of critical heat flux, q_{CHF}, with inlet subcooling, $DT_{s,i}$, or outlet (local) subcooling, $DT_{s,o}$, for different pressures. Figure 2 exemplifies the variations of q_{CHF} with subcooling for different mass fluxes. As seen, for similar pressure or similar mass flux the CHF increases as subcooling increasing. At lower pressure the trend of q_{CHF} with $DT_{s,i}$ is steeper. While when the pressure exceeds 18

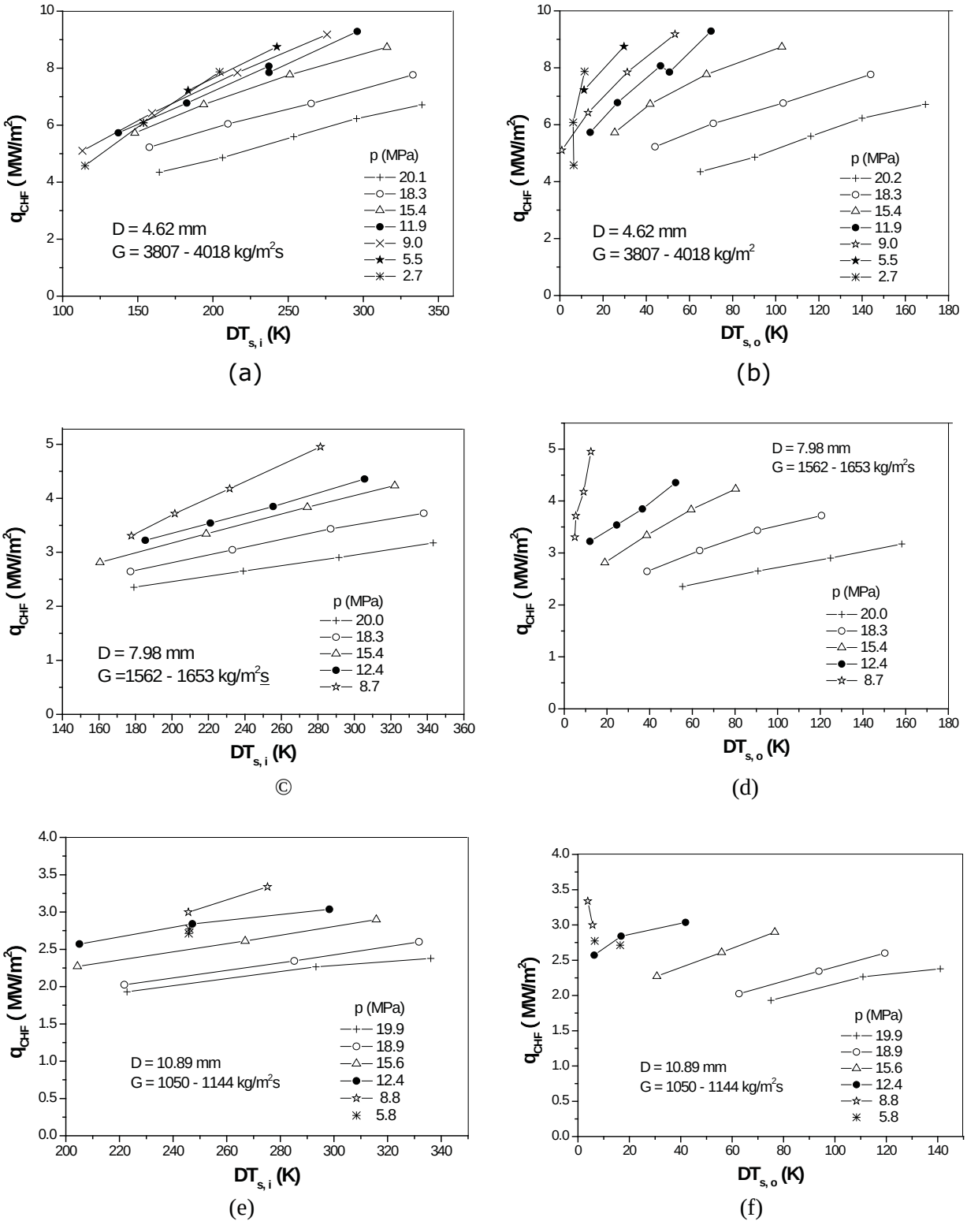

Figure1- Effect of pressure on the CHF for higher pressures

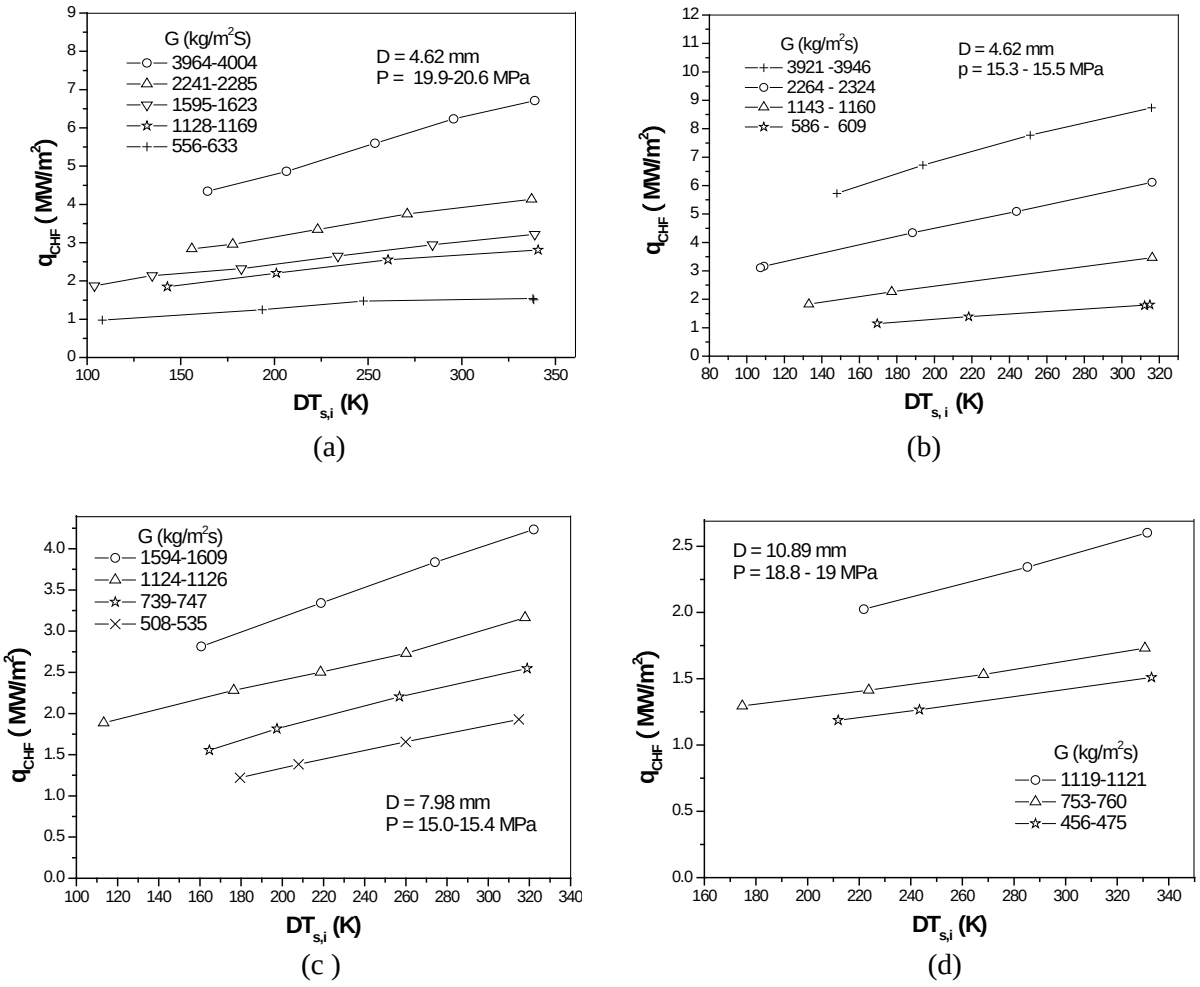

Figure 2 – Effect of mass flux on the CHF for higher pressure

MPa the trend of q_{CHF} with subcooling becomes weak distinctly, and the q_{CHF} is much lower than lower pressure due to the substantial decrease in the surface tension.

It is widely accepted that at low subcooling the CHF is induced by a limit of enthalpy of bubbly-layer [12 -14], while at high subcooling it is induced by a limit of bubbly-layer condensation [15-17]. This suggests that the CHF with higher local subcooling is dominated by the local condition, and the CHF with lower local subcooling is dominated by the total upstream power. The former one is observed from the experiment with nearly the same diameter but different heated length [1, 9, 10]. The latter is observed in figure 1(e) and (f) for the two data points with P = 5.80 MPa, in which very small differences in the q_{CHF} and $DT_{s,i}$ result in some difference in $DT_{s,o}$, indicating that the $DT_{s,o}$ is not dominant to the CHF for low local subcooling.

The effect of diameter on the CHF is illustrated in figure 3. For similar pressure and mass flux with $DT_{s,o}$> 30 K higher CHF is obtained in smaller tube. This result was also observed by the authors and other investigators, though the extent of this effect was different for different conditions [1].

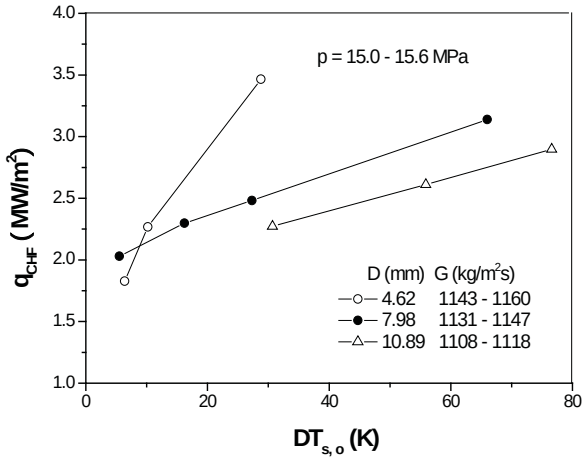

Figure 3 - Effect of diameter on the critical heat flux for higher pressure

3.2 Lower Pressure

The experimental conditions for lower pressure in tubes of D_i = 2.32, 5.16, 8.05, 10.0 and 16.0 mm are listed in Table 2.

Figure 4 and 5 exemplify the variations of the CHF with local subcooling for similar pressure and similar velocity, respectively. As seen, the CHF decreases with local subcooling decreasing. When the local

Table 2 - The experimental conditions for lower pressures

No.	Diameter D_i (mm)	Heated length L_h (mm)	Pressure P (MPa)	Velocity V (m/s)	Subcooling $\Delta T_{s,o}$ (K)	q_{CHF} (MW/m^2)	Number of data
1	2.32	98	0.10– 1.68	4.35 – 23.3	3.7 – 100.9	11.6-38.3	112
2	5.16	255	0.13-1.78	2.59-22.3	6.2-89.6	8.4-29.3	63
3	8.05	383, 396	0.14-1.92	1.88-15.9	8.3 – 88.2	4.7-17.9	65
4	10.0	295, 400	0.15-1.66	3.39-9.26	30.3-89.5	4.4-10.9	53
5	16.0	295, 390	0.19-1.29	1.47-13.4	36.7 -108.7	4.2-14.6	56

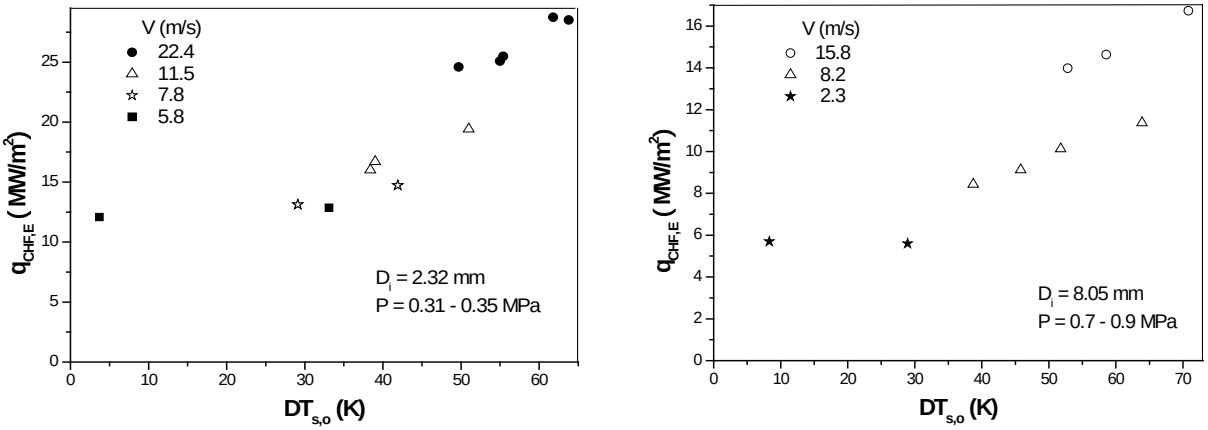

(a) (b)

Figure 4 – Effect of velocity on the CHF for lower pressure

subcooling is less than 30 – 40 K the trend of CHF with local subcooling appears different from higher subcooling. In particular, at the pressure of less than 0.3 MPa with low subcooling the flow resistance is increased significantly due to larger bubble size. At this condition the trend of CHF with $DT_{s,o}$ becomes weak or negative, as also observed in reference [11]. Figure 6 illustrates the effect of diameter on the CHF. For the present conditions the diameter has negative effect on the CHF, as in higher pressure.

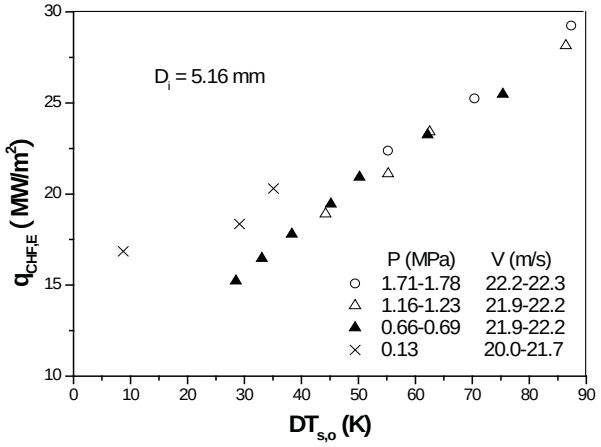

Figure 5 – Effect of pressure on the CHF for lower pressure

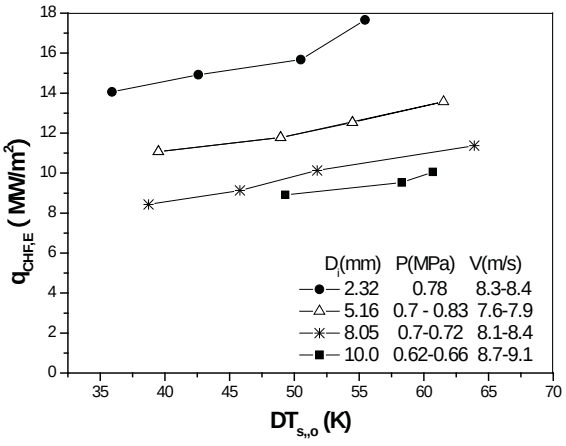

Figure 6 – Effect of diameter on the CHF for lower pressure

4. FORMULATIONS OF THE EXPERIMENTAL RESULTS

In the previous study the experimental data of D = 7.98 mm were formulated by the following empiric correlation [10],

$$q_{CHF} = cq_s \tag{1}$$

where q_s is the heat flux for the exit to reach the saturation temperature, evaluated by

$$q_s = \frac{(H_s - H_i)GD_i}{4L_h}$$

and

$$c = Min\left[2350(1-0.0307p)(G(H_s - H_i))^{-0.35}, 1.0\right] \tag{2}$$

where p is the pressure in MPa, H_i and H_s the inlet enthalpy and saturation enthalpy in J/kg, respectively, G the mass flux in kg/m^{2}s, D_i the inner diameter and L_h the heated length in m.

For calculations of the experimental results with the data of D_i = 4.62 and 10.89 mm, the formulation (2) is modified as

$$c = Min\left[2350(1-0.0307p)(G(H_s - H_i))^{-0.35}(D_i / 0.008)^{-0.35}, 1.0\right] \tag{3}$$

The calculation results of the experimental data are shown in figure 7. The deviations of more than 90% of the data points are less than 10%. The AVG are +1.1, +0.7 and -2.1%, and the RMS are 7.15, 5.35 and 5.70% for D_i=4.62, 7.98 and 10.89mm, respectively.

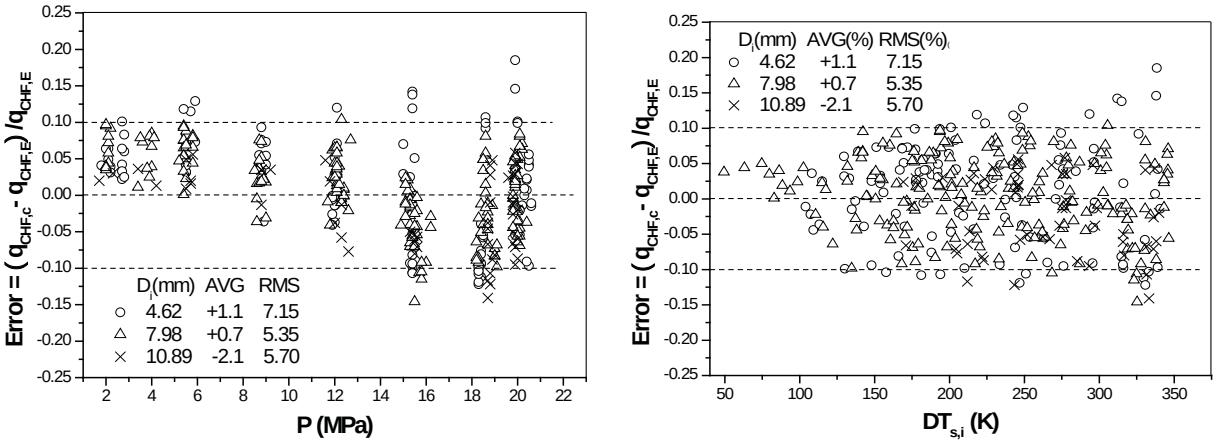

(a) (b)

Figure 7 Comparison of the experimental results with the calculations of formulation for higher pressure

4.2 Lower Pressure

It is recognized that for the subcooled critical heat flux with L_h > 200 mm the effect of heated length on the CHF disappears [6, 7, 18]. For the tube of D = 2.32 mm the heated length is smaller, but the ratio of L_h/D_i exceeds 40. Therefore, the effect of heated length is negligible for these five tubes.

For the data of D_i = 2.32, 5.16, 8.05, 10.0 and 16.0 mm, except of those of $DT_{s,o}$ < 35 K, an empirical correlation was proposed, as

$$q_{CHF} = 0.108(1+0.104V)(15P+DT_{s,o}^{1-0.1P})(\frac{D_i}{0.008})^{-0.35} \quad (4)$$

where the critical heat flux q_{CHF} is in MW/m^2, velocity V in m/s, pressure p in MPa, local subcooling $DT_{s,o}$ in K and inner diameter D_i in m. The effect of diameter on the CHF is the same as in the higher pressure. For these data the calculation results are shown in figure 8. Totally, for $DT_{s,o}$ > 35 K the 301

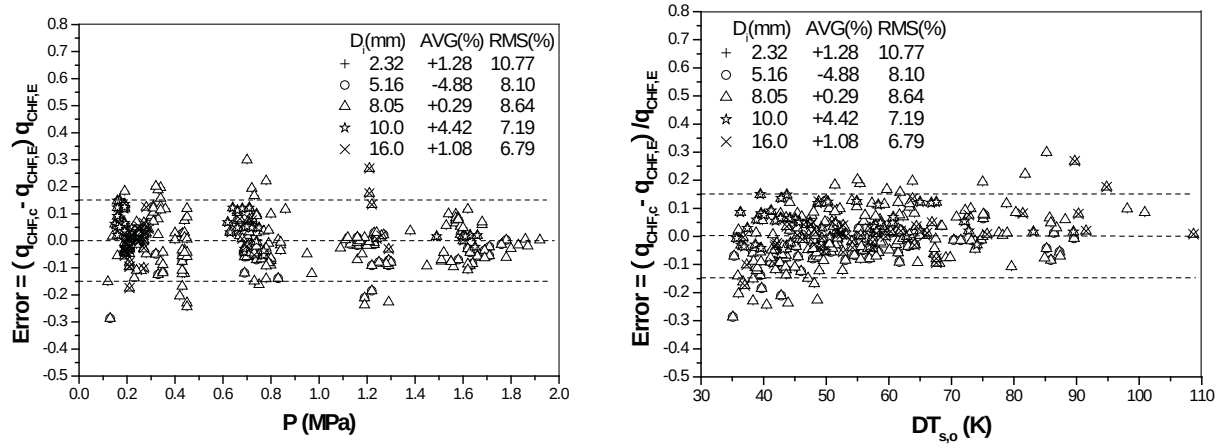

(a) (b)

Figure 8 Comparison of the experimental data with calculations of equation (1) and (4) for lower pressure

data points are calculated with the deviation of less than 15%. The AVG is +1.28, -4.88, +0.29,+4.42 and +1.08 %, and the RMS is 10.77, 8.10, 8.64, 7.19 and 6.79% for D_i = 2.32, 5.16, 8.05, 10.0 and 16.0 mm, respectively.

5. PHYSICAL MODEL

For subcooled flow boiling CHF two types of physical models have been proposed, based on the assumptions of different mechanisms for different conditions: i) the critical enthalpy models for low subcooling, in which the CHF is induced by a limit of the enthalpy of bubbly layer [12 - 14], and ii) the liquid sublayer dryout model for high subcooling, in which the CHF is induced by a limit of heat transfer capability from the edge of bubbly layer to the subcooled liquid core [15 - 17]. At high subcooling the thickness of bubbly layer is determinant, and it is evaluated by the diameter of single bubble detached from the surface, multiplying a constant. For extending this model to lower subcooling condition, in the author's previous investigation the thickness of bubbly layer was modified to account for the bubble crowding. The reader refers to the previous paper for details [11]. The major equations of the model are represented in this paragraph.

The thickness of bubbly layer, δ, is as

$$\delta = k_1 D_B (1 + k_2 e^{-k_3 \Pr Q}) \tag{5}$$

where the Pr is the Prandtl number, Q is a parameter group (see Eq.(12)), and the factors k_1, k_2 and k_3 are constants, as k_1 = 0.75, k_2 =1.0×10^3, and k_3 = 1.0. At low subcooling the critical heat flux is close to q_s, and not sensitive to the δ, thus the maximum value of δ is simply set as 0.1D_i.

The D_B is the bubble or vapor blanket equivalent diameter, evaluated by [15]

$$D_B = \frac{32\sigma f(\beta)\rho_L}{fG^2} \tag{6}$$

where σ is the surface tension, ρ_L the liquid density and G the mass flux. The $f(\beta)$ is a function relative to the contact angle with surface. In the previous study it is represented by

$$f(\beta) = 0.03 \qquad \text{for} \quad p \le 10MPa$$

and

$$f(\beta) = 0.03(1 - 0.055(p - 10)) \qquad \text{for} \quad p > 10MPa \tag{7}$$

where p is the pressure in MPa. In the present investigation it is applied for D_i,> 4 mm. But for D_i = 2.32 mm the $f(\beta)$ is modified as

$$f(\beta) = 0.03(1 + 1.5/D_i) \tag{8}$$

The friction factor, f, is calculated by Colebrook-White equation combined with Levy's rough surface model [19], as

$$\frac{1}{\sqrt{f}} = 1.14 - 2.0\log\left(\frac{\varepsilon}{D_i} + \frac{9.35}{\mathrm{Re}\sqrt{f}}\right) \tag{9}$$

where D_i is the tube diameter, Re the Reynolds number, and ε the surface roughness, accounted by $\varepsilon = 0.75 D_B$.

In the liquid core the velocity is represented by the Karman distribution, as

$$\begin{aligned} U^+ &= y^+ && 0 \le y^+ < 5 \\ U^+ &= 5.0 \ln y^+ - 3.05 && 5 \le y^+ < 30 \\ U^+ &= 2.5 \ln y^+ + 5.5 && y^+ \ge 30 \end{aligned} \tag{10}$$

The temperature distribution is represented by [20]

$$\begin{aligned} T_0 - T &= Q \,\mathrm{Pr}\, y^+ && 0 \le y^+ < 5 \\ T_0 - T &= 5Q\left\{ \mathrm{Pr} + \ln\left[1 + \mathrm{Pr}\left(\frac{y^+}{5} - 1\right)\right]\right\} && 5 \le y^+ < 30 \\ T_0 - T &= 5Q\left[\mathrm{Pr} + \ln(1 + 5Pr) + 0.5 \ln\left(\frac{y^+}{30}\right)\right] && y^+ \ge 30 \end{aligned} \tag{11}$$

with

$$Q = \frac{q}{\rho_l C_{pL} U_\tau} \tag{12}$$

The T_0 is a referent value, determined by $T = T_s$ at $y = \delta$.

The calculation of model is based on the heat balance equation, as

$$H = H_i + \frac{4qL_h}{GD_i}$$

where H_i is the inlet enthalpy and L_h the heated length. The H is the local enthalpy, represented by

$$H\,\dot{m} = H_C(\dot{m} - \dot{m}_{B,g} - \dot{m}_{B,l}) + H_g\,\dot{m}_{B,g} + H_l\,\dot{m}_{B,l} \tag{13}$$

where $\dot{m}$ is the total flow rate, $\dot{m}_{B,g}$ and $\dot{m}_{B,l}$ are the vapor and liquid flow rate in the bubbly layer, respectively, H_g and H_l are the vapor and liquid enthalpy, and H_C is the enthalpy of liquid core, calculated from the average temperature T_C, as

$$T_C = \frac{\int_\delta^R TU(r-y)dy}{\int_\delta^R U(r-y)dy}$$

where R is the radius of tube, and δ is the distance from wall at which the temperature is equal to the saturation value.

The $\dot{m}$, $\dot{m}_{B,g}$ and $\dot{m}_{B,l}$ are evaluated by

$$\dot{m} = \frac{\pi D_i^2}{4} G$$

$$\dot{m}_{B,g} = \pi(D_i - \delta)\delta\alpha_B \rho_g \overline{U_B}$$

and

$$\dot{m}_{B,L} = \pi(D_i - \delta)\delta(1 - \alpha_B)\rho_l \overline{U_B}$$

where α_B is the void fraction in the bubbly layer, and it is taken as α_B = 0.9. $\overline{U_B}$ is the average velocity of bubbly layer, estimated by

$$\overline{U_B} = 0.5 U_{y=\delta}$$

The calculation is started with a test heat flux q ($q < q_s$), and the result of CHF is obtained through an iterative process.

.

For higher and lower pressure the comparison of the calculations of the physical model with the experimental data are shown in figure 9 and 10 by displaying the $Error = (q_{CHF,C} - q_{CHF,E}) / q_{CHF,E}$ versus P and $DT_{s,i}$ or $DT_{s,o}$. For higher pressure the AVG is -1.2, +0.12 and +1.4%, and the RMS is 5.37, 4.86 and 6.86% for D_i = 4.62, 7.98 and 10.89 mm, respectively. For lower pressure the AVG is +1.83, -4.10, +2.28, +5.88 and +5.23%, and the RMS is 7.37, 7.46, 5.29, 7.28 and 8.60%, for D_i = 2.32, 5.16, 8.05, 10.0 and 16.0 mm, respectively.

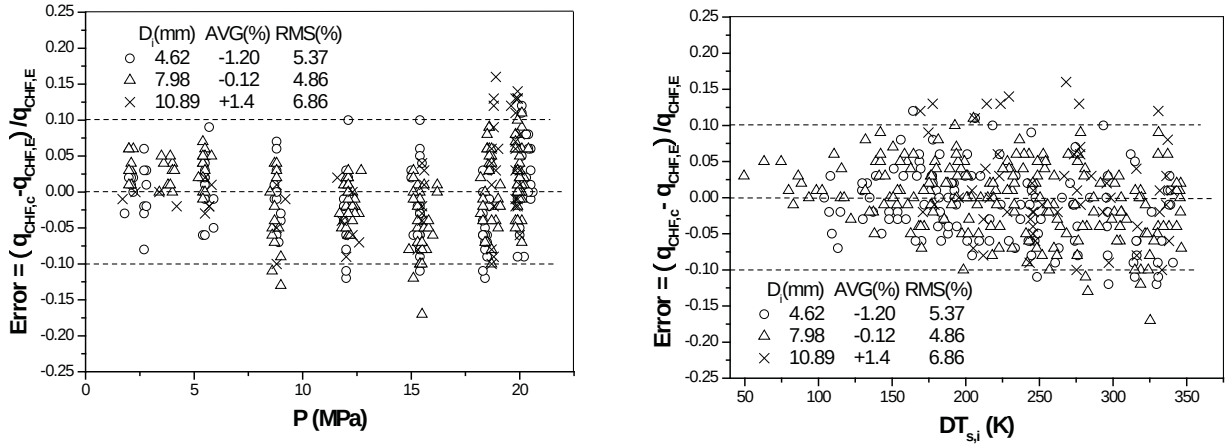

(a) (b)

Figure 9 - Comparison of the calculations of model with the experimental data for higher pressure

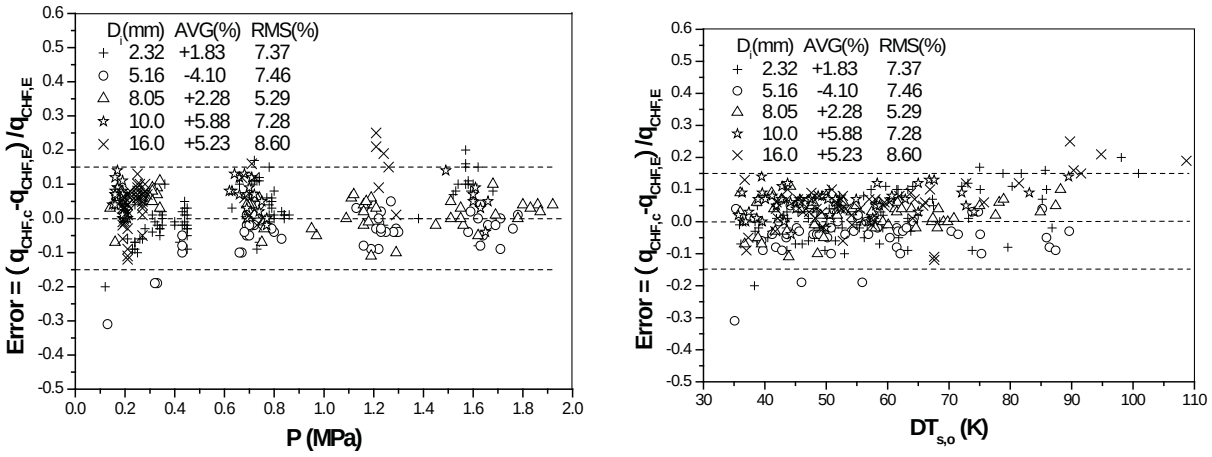

(a) (b)

Figure 10 Comparison of the calculations of model with the experimental data for lower pressure

6. CONCLUSIONS

The subcooled flow CHF experiment is conducted in Inconel-625 tubes of D_i = 4.62, 7.98 and 10.89 mm in diameter with water flowing upward to cover the ranges of pressure of 1.7 to 20.6 MPa, mass flux of

454 – 4055 kg/m^{2}s and inlet subcooling of 53 – 361 K. It is also extended to lower pressure in tubes of D_i = 2.32 to 16.0 mm with pressure of 0.1 – 1.92 MPa, velocity of 1.47 to 23.3 m/s and critical heat flux of up to 38.3 MW/m^2. The effects of the parameters are studied systematically. The major conclusions are achieved as follows:

- The mass flux has strong effect on the critical heat flux. The effect of subcooling on the CHF is closely related to the pressure. At lower pressure the CHF increases distinctly with subcooling increase. While as the pressure increases this effect is decreased. When the pressure is higher than 18 MPa the trend is weak, and much lower CHF is obtained.
- The critical heat flux increases as the diameter decreases, and it is accounted by $q_{CHF} \propto D_i^{-0.35}$ for both the higher pressure and lower pressure.
- The empiric correlations and a physical model are proposed to calculate the CHF properly for the pressure from atmosphere to the near-critical point and wide range of mass flux.
- At higher local subcooling the CHF is determined by the local conditions, and at lower local subcooling the CHF is determined by the upstream condition. For lower subcooling or low quality the CHF characteristics will be studied further.

7. REFERENCES

[1] Thermohydraulic Relationships for Advanced Water Cooled Reactors, IAEA-TECDOC 1203, 2001

[2]. B.R. Vijayarangan, S. Jayanti, A.R. Balakrishan, "Studies on critical heat flux in flow boiling at near critical pressures", *Int. J. Heat and Mass Transfer*, Vol. 49, pp. 259 – 268 , 2006.

[3] S. D. Hong, S. Y. Chun, S. Y. Kim and W. P. Beak, "Heat Transfer Characteristics of an Internally Heated Annulus Cooled with R-134a near the Critical Pressure", J. Korean Nuclear Society, Vol. 36, No. 5, pp. 403-414, 2004.

[4] S.Y. Chun, S.D. Hong, H. Kikura and M. Aritomi, "Critical Heat Flux in a Heater Rod Bundle Cooled by R-134a Fluid near the Critical Pressure", Nucl. Science and Technology, Vol. 44, No. 9, pp. 1189 – 1198, 2007.

[5] S. T. Yin, T. J. Lui, Y. D. Huang and R. M. Tain, "Measurements of Critical Heat Flux in Forced Flow at Pressures up to the Vicinity of the Critical Point of Water", Proc. of 1988 National Heat Transfer Conference in USA, Vol. 1, pp. 501-506, 1988.

[6] Y. Chen, L. Zhou and C. Yang, "Subcooled Boiling Critical Heat Flux in Annuli at Lower Pressure", Proc. NUTHOS-5, Japan, 2004.

[7] Y. Chen, H. Zhang, , F. Guo and L. Hao, "Subcooled Flow Boiling CHF in Tubes with Different Diameters", Presented at Boiling 2000, Alaska, 2000.

[8] Y. Chen, C. Yang, and Y. Mao, "An Experimental Study of Subcooled Flow Boiling Critical Heat Flux of Water under Steady-State and Flow-Transient Conditions at Lower Pressure", Proc of. the 11th Int. Topical Meeting on Nuclear Reactor Thermal-Hydraulics (NURETH-11), paper-459, Avignon, France, 2005.

[9] Y. Chen, C. Yang, M. Zhao, K. Bi, K. Du and S. Zhang "An Experimental Study of Critical Heat Flux in a tube for Near-critical Pressures," Proc. of the 5th Int. Sym. SCWR (ISSCWR-5), Vancouver, Canada, 2011.

[10] Y. Chen, C. Yang, M. Zhao, K. Bi, K. Du and S. Zhang, "Subcooled Boiling Critical Heat Flux of Water Flowing Upward in a Tube for Lower Flow and Pressure up to 20 MPa", Proc. of the 14th International Topical Meeting on Nuclear Reactor Thermal Hydraulics (NURETH-14), p-620, Ontario, Canada, 2011.

[11] Yuzhou Chen, Critical Heat Flux in Subcooled Flow Boiling of Water, Chapter 9, in An Overview of Heat Transfer Phenomena, Edited by Salim N, Kazi, INTECH, 2012
[12] L.S. Tong and Y.S. Tang, "Boiling Heat Transfer and Two-Phase Flow", Taylor & ISBN 1-56032-485-6 Francis,1997.
[13] J. Weisman and B. S. Pei, "Prediction of Critical Heat Flux in Flow Boiling at low qualities", Int. J. Heat Mass Transfer, Vol. 26, pp.1463 – 1477, 1983.
[14] L. S. Tong, "Boundary Layer Analysis of the Flow Boiling Crisis", Int. J. Heat Mass Transfer, Vol. 11, pp. 1208 – 1211, 1968.
[15] G. P. Celata, M. Cuma, A Mariani, M. Simosini and G Zummo, "Rationalization of Existing Mechanistic Models for the Prediction of Water Subcooled Flow Boiling Critical Heat Flux", Int. J. Heat and Mass Transfer Vol. 37, Suppl. 1, pp. 347-360, 1994.
[16] Y. Katto, "A Prediction Model of Subcooled Water Flow Boiling CHF for Pressures in the Region 0.1-20.0 MPa", Int. J. Heat ans Mass Transfer, Vol. 35, pp. 1115-1123, 1992.
[17] C. H. Lee and I. Mudawar, "A Mechanistic Critical Heat Flux Model for Subcooled Flow Boiling Based on Local Bulk Flow Conditions", Int. J. Multiphase Flow, Vol. 14, pp. 711-728, 1983.
[18] V.L. Tolubinsky, A.K. Litoshenkp and V.L. Shevtsov, "Heat Transfer Crisis at Water Boiling in Annular Channels with External and Internal Heating", Heat Transfer 1970, Vol. YI, B6.11, 1970.
[19] S Levy, "Forced Convection Subcooled Boiling – Prediction of Vapor Volumetric Fraction", Int. J. Heat Mass Transfer, Vol.10, pp. 951 – 965, 1967.
[20] R.C. Martinelli, "Heat Transfer in Molten Metals", Trans. ASME 69, pp. 947-951,1947.